Progress In Electromagnetics Research, Vol. 156, 105–133, 2016

Pathological Brain Detection by Artificial Intelligence in Magnetic Resonance Imaging Scanning

Shuihua Wang[1, 2, 3, #], Yin Zhang[4, #], Tianmin Zhan[5, #], Preetha Phillips[6], Yudong Zhang[1, 2, *], Ge Liu[7], Siyuan Lu[1, 8], and Xueyan Wu[1, 9]

(*Invited Review*)

Abstract—(Aim) Pathological brain detection (PBD) systems aim to assist and even replace neuroradiologists to make decisions for patients. This review offers a comprehensive and quantitative comparison for PBD systems by artificial intelligence in magnetic resonance imaging (MRI) scanning. (Method) We first investigated four categories of brain diseases, including neoplastic disease, neurodegenerative disease, cerebrovascular disease, and inflammation. Next, we introduced important MRI techniques, such as the shimming, water and fat suppression, and three advanced imaging modalities (functional MRI, diffusion tensor imaging, and magnetic resonance spectroscopic imaging). Then, we discussed four image preprocessing techniques (image denoising, slice selection, brain extraction, spatial normalization, and intensity normalization), seven feature representation techniques (shape, moment, wavelet, statistics, entropy, gray level co-occurrence matrix, and Fourier transform), and two dimension reduction techniques (feature selection and feature extraction). Afterwards, we studied classification related methods: six learning models (decision tree, extreme learning machine, k-nearest neighbors, naive Bayes classifier, support vector machine, feed-forward neural network), five kernel functions (linear, homogeneous and inhomogeneous polynomial, radial basis function, and sigmoid), and three types of optimization methods (evolutionary algorithm, stochastic optimization, and swarm intelligence). (Results) We introduced three benchmark datasets and used K-fold stratified cross validation to avoid overfitting. We presented a detailed quantitative comparison among 44 state-of-the-art PBD algorithms and discussed their advantages and limitations. (Discussions) Artificial intelligence is now making stride in the PBD field and enjoys a fair amount of success. In the future, semi-supervised learning and transfer learning techniques may be potential breakthroughs to develop PBD systems.

1. INTRODUCTION

The magnetic resonance imaging (MRI) is the most popular method for brains, since it provides clearer soft tissue details than traditional neuroimaging techniques. Nevertheless, the manual interpretation on MR images is tedious due to the large amount of imaging data, with the professional name of "*curse of dimensionality*" [1]. To solve the problem, the pathological brain detection (PBD) was proposed in the last decade [2]. It becomes a computer-aided diagnosis (CAD) system and focuses on MR images. The aim of PBD is to help neuroradiologists to make decisions based on brain images.

Received 8 July 2016, Accepted 16 August 2016, Scheduled 23 August 2016

* Corresponding author: Yudong Zhang (zhangyudong@njnu.edu.cn). # Those authors contribute equally to this paper.

[1] School of Computer Science and Technology, Nanjing Normal University, Nanjing, Jiangsu 210023, China. [2] School of Electronic Science and Engineering, Nanjing University, Nanjing, Jiangsu 210046, China. [3] Department of Electrical Engineering, The City College of New York, CUNY, New York, NY 10031, USA. [4] School of Information and Safety Engineering, Zhongnan University of Economics and Law, Wuhan, Hubei 430073, China. [5] School of Computer Science & Communications Engineering, Jiangsu University, Zhenjiang, Jiangsu 212013, China. [6] School of Natural Sciences and Mathematics, Shepherd University, Shepherdstown, WV 25443, USA. [7] Department of Computer Science, Tennessee State University, Nashville, TN 37209, USA. [8] State Key Lab of CAD & CG, Zhejiang University, Hangzhou, Zhejiang 310027, China. [9] Key Laboratory of Statistical Information Technology and Data Mining, State Statistics Bureau, Chengdu, Sichuan 610225, China.

At present, two types of PBD systems exist. Type I is aimed for detecting all types of brain diseases, and its detection rate can be improved gradually. Type II is aimed for detecting each specific brain disease and then integrates all these systems together. Both types of systems are of hot research topics.

The development of PBD can be divided into three stages: From 1990s, based on the knowledge and experiences obtained from the neuroradiologists [3], computer scientists developed PBD by the so-called "knowledge-based systems" or "expert systems" techniques [4]. The employed features are commonly human understandable, such as cortical thickness, area of particular brain tissue, etc. Ref. [3] developed an expert system for differential diagnosis of acute stroke. [5] presented an expert system "*Focus*" for locating the acute neurologic events. [6] developed the "EPEXS" for evoked potential analysis and interpretation. [7] compared expert systems with human expertise, and at an abstract level proved that they complemented each other. [8] developed an expert system that detected cerebral blood flow (CBF) deficits in neuropsychiatric disorders.

Later, computer scientists realized mathematical features (shape, texture, statistical, etc.) can also achieve equivalent or even better performances than human-understandable features. Therefore, scholars tend to add advanced image features such as wavelets and gray-level occurrence matrix (GLCM). [9] used wavelet compression technique to detect brain lesions. [10] used 3D wavelet representation for tissue segmentation. [11] employed GLCM to lateralize seizure focus in temporal lobe epilepsy (TLE) patients with normal volumetric MRI.

Moreover, the successes of pattern recognition (PR) in other fields also suggest the scholars to use PR techniques to detect pathological brains. PR systems with labeled training data are called "*supervised learning (SL)*" [12], and those with no labeled data are called "*unsupervised learning*" [13]. SL is commonly used in PBD, since neuroradiologists can label the data.

Recently, various optimization techniques have also been proposed and applied to train the classifier to increase the detection performance. Traditional classifier training was gradient descent based methods [14]; nevertheless, the complicated optimization surfaces and discretized version of the problem make gradient-based methods suffer from falling into local best points and basins. Hence, new meta-heuristic optimization methods were proposed. [15] proposed ant colony optimization (ACO) algorithm based on ant colony. [16] proposed particle swarm optimization (PSO) algorithm based on bird flocking. Besides, differential evolution (DE) [17], artificial bee colony [18], glowworm swarm optimization (GSO) [19], and many excellent optimization techniques were proposed.

Figure 1 shows a block diagram of developing a PBD by AI in MRI. Roughly, we can divide the process into eight steps: diagnosis, MRI techniques, image preprocessing, feature representation, dimension reduction, classification, kernel, and optimization methods. In what follows, we will expatiate each block.

Figure 2 shows the curve of related publications every year. The results show that the researches on this topic are increasing apparently and steadily over time. Moreover, this picture also validates

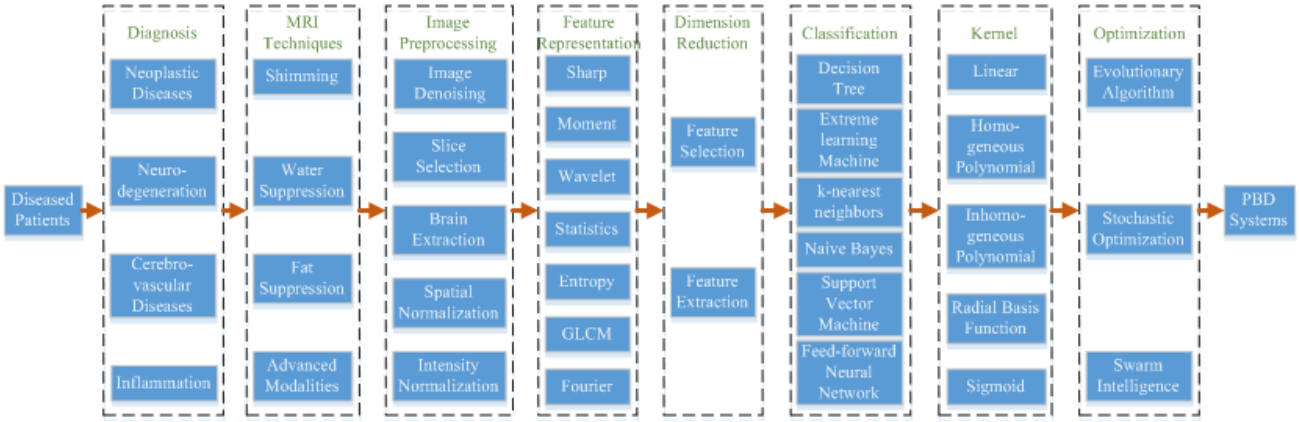

Figure 1. Block diagram of developing a PBD.

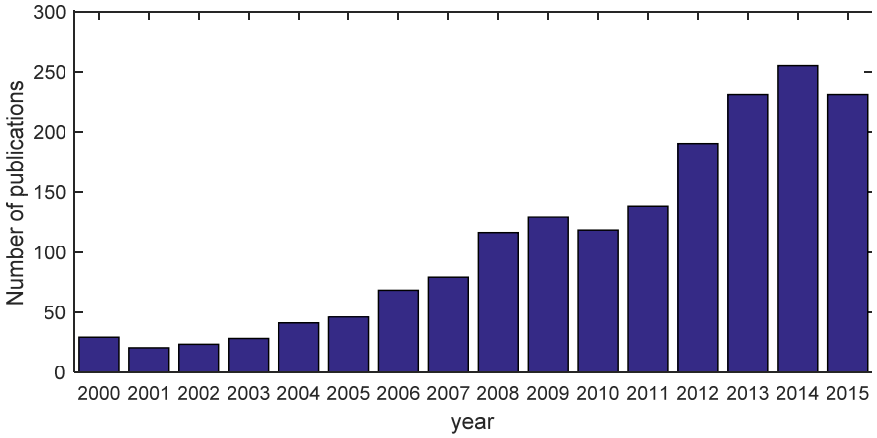

Figure 2. Publications versus year.

Table 1. Four categories of brain diseases.

Category	Common diseases
Neoplastic disease	glioma, metastatic bronchogenic carcinoma, meningioma, sarcoma, astrocytoma, oligodendroglioma, metastatic adenocarcinoma,
Neurodegeneration	Parkinson's disease, Alzheimer's disease, Huntington's disease, motor neuron disease (amyotrophic lateral sclerosis), Pick's disease, cerebral calcinosis, Batten disease, prion disease, spinocerebellar ataxia, Friedreich's ataxia
Cerebrovascular disease	cerebral hemorrhage, acute stroke, hypertensive encephalopathy, multiple embolic infarction, subacute stroke, vascular dementia, chronic subdural hematoma, cavernous angioma, subarachnoid hemorrhage, fatal stroke, transient ischemic attack
Inflammation	encephalitis, cerebral Toxoplasmosis, multiple sclerosis, abscess, Lyme encephalopathy, AIDS dementia, Herpes encephalitis, Creutzfeldt-Jakob disease, meningitis, vasculitis

that the AI applied to PBD receives the attention of scholars, and it will attract more scholars to participate in this field. This work aims to give a comprehensive review on PBD by AI in MRI technique. In Section 2, we categorize and present common brain diseases. Section 3 gives principles of data acquisition. Section 4 offers the preprocessing techniques, summarizes the image features, and discusses the dimension reduction techniques. Section 5 introduces the classifiers, kernel methods and training methods. Section 6 compares 44 state-of-the-art PBD methods and gives future directions. We implemented this survey based on literature in Web of Science Core Collection, IEEE Explorer, and Scopus.

2. BRAIN DISEASES

A mass of brain diseases exist. Roughly, we can divide them into four categories.

Neoplastic disease: First is neoplastic disease (also called tumor). The primary neoplastic disease starts in brain and remains therein [20], while the secondary starts elsewhere and then travels to the brain [21]. Benign tumors do not have cancer cells, rarely spread, and may cause problems if pressing certain brain areas. Malignant tumors have cancer cells and invade healthy tissues nearby.

Four grades of brain tumors are listed in Table 2. Grade I tumors are rare in adults and associated with long-term survival. Grade II tumors sometimes spread into nearby tissues and may come back as a higher-grade tumor. Grade III and IV tumors actively reproduce abnormal cells. Grade IV tumors are extremely dangerous: they form new blood vessels to maintain rapid growth and contain necrosis in their center. Effective treatments include surgery [22], radiation therapy [23], chemotherapy [24], and combined therapies [25].

Neurodegeneration: The second category is neurodegeneration, viz., the progressive loss (even death) in structure or function of neurons [26]. Neurons normally do not reproduce, so they cannot be updated after being damaged [27]. Neurodegeneration diseases are incurable and lead to progressive degeneration. They affect many daily activities and structures: muscle [28], movement [29], balance [30], talking, heart function [31], sleep [32], etc. It also causes problems in mental functioning [33].

Cerebrovascular Disease: The third category is cerebrovascular disease. It is a severe medical condition, caused by affecting blood supply to the brain. Globally, the cardiovascular disease is

Table 2. Four grades of brain tumors.

	Grow speed	Look under a microscope
Grade I	slow	almost normal
Grade II	relatively slow	slightly abnormal
Grade III	relatively fast	abnormal
Grade IV	fast	very abnormal

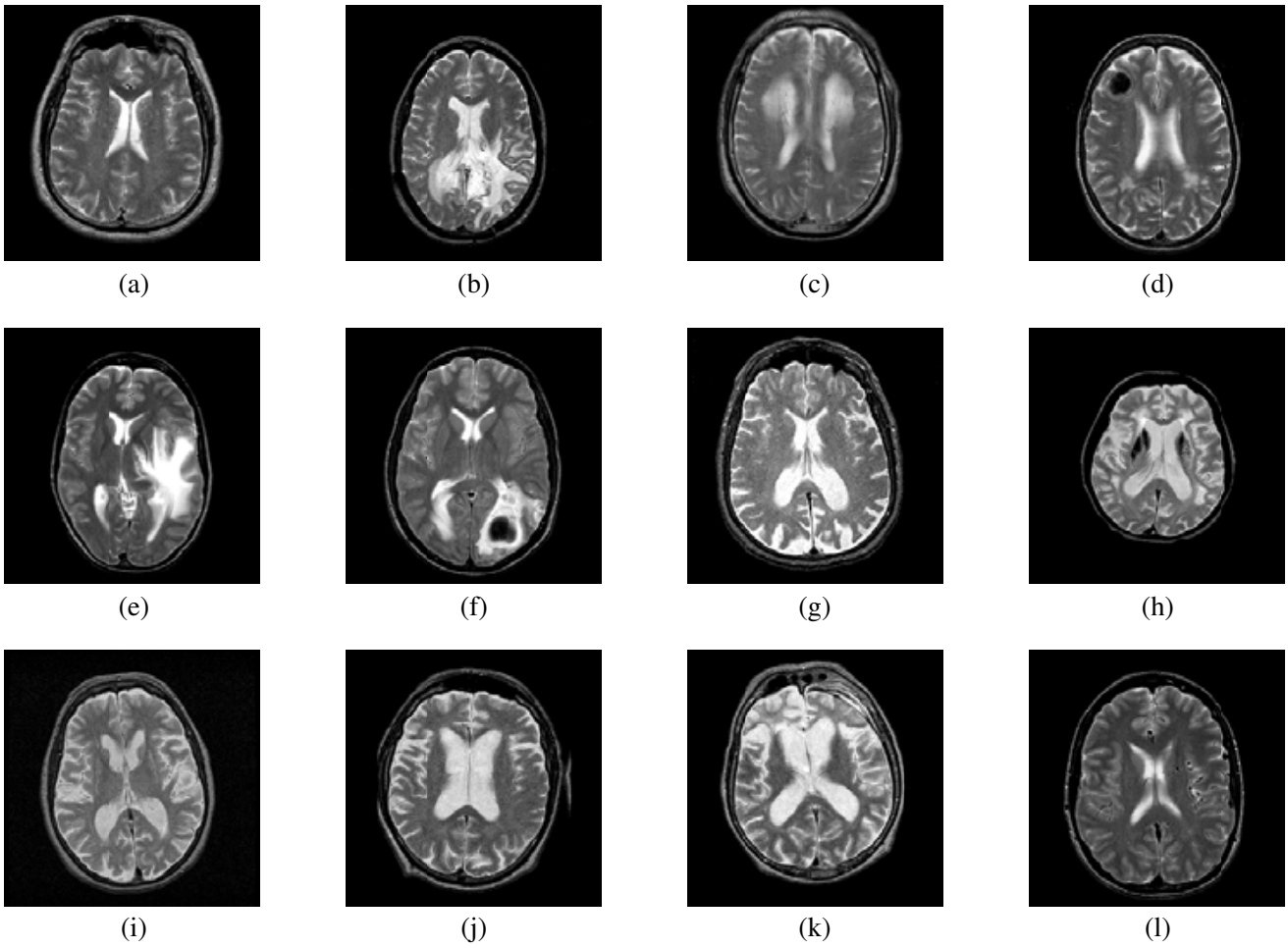

(a) (b) (c) (d)

(e) (f) (g) (h)

(i) (j) (k) (l)

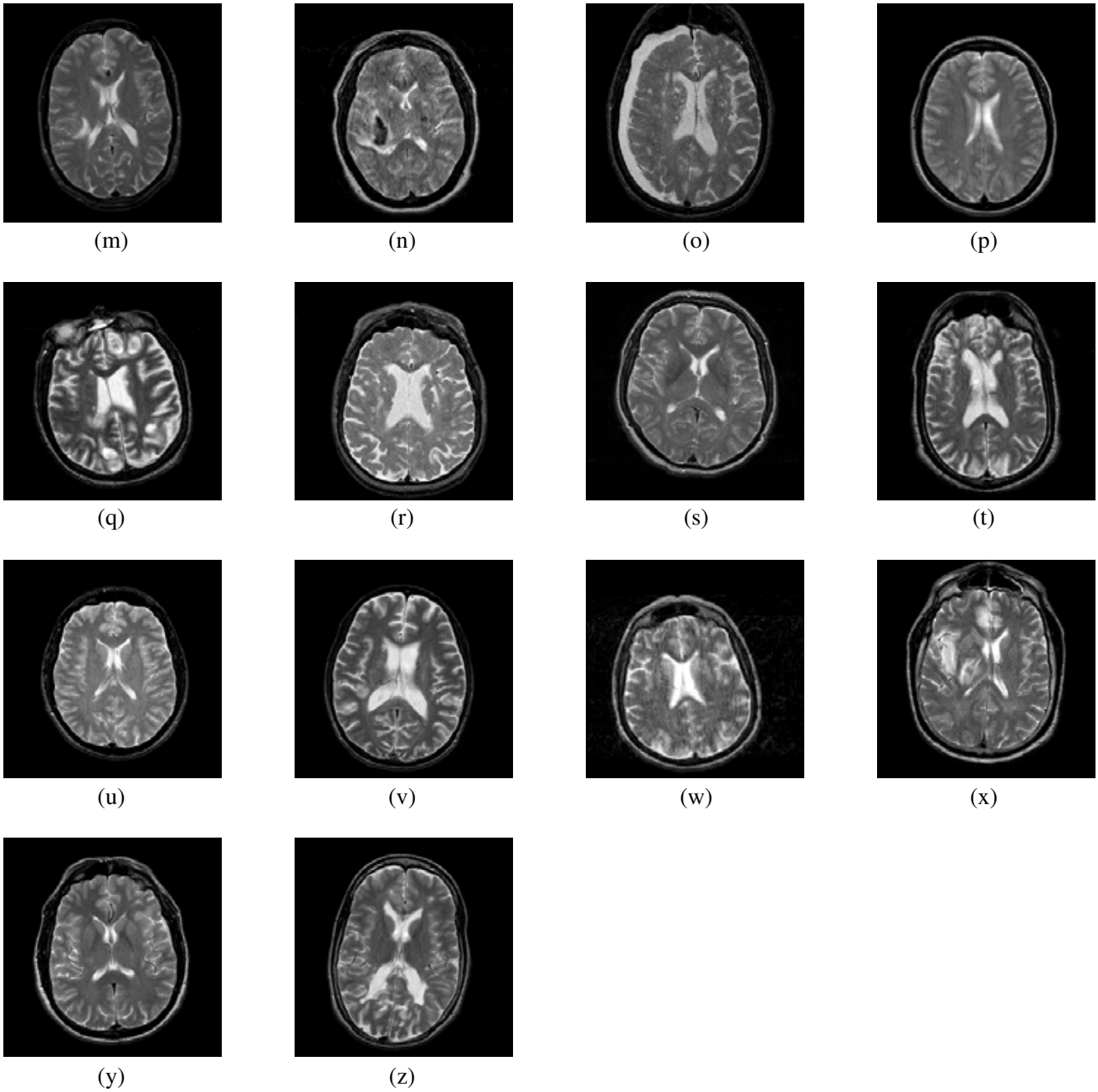

Figure 3. Illustration of typical brain diseases in MRI view. (a) Healthy brain. (b) Glioma. (c) Meningioma. (d) Metastatic adenocarcinoma. (e) Metastatic Bronchogenic Carcinoma. (f) Sarcoma. (g) Alzheimer's disease. (h) Cerebral calcinosis. (i) Huntington's disease. (j) Motor Neuron disease. (k) Pick's disease. (l) Arteriovenous malformation. (m) Cavernous angioma. (n) Cerebral hemorrhage. (o) Chronic subdural hematoma. (p) Hypertensive encephalopathy. (q) Multiple embolic infarctions. (r) Vascular dementia. (s) Acute stroke. (t) Subacute stroke. (u) AIDS dementia. (v) Cerebral Toxoplasmosis. (w) Creutzfeldt-Jakob disease. (x) Herpes Encephalitis. (y) Lyme encephalopathy. (z) Multiple sclerosis.

responsible for more deaths than any other diseases. Four common cerebrovascular diseases are introduced: (i) A stroke happens when the blood supply is blocked or interrupted by a clot, then parts of the brain die due to cerebral infarction [34]. (ii) A transient ischemic attack (TIA) is caused

by temporary blood disruption [35]. It is also called a "mini-stroke" with symptoms resolved within 24 hours [36]. (iii) Subarachnoid hemorrhage (SAH) happens when blood leaks from arteries, located underneath the arachnoid, to the brain surface [37]. (iv) Vascular dementia is caused by brain cell damage due to a complex interaction of cerebrovascular diseases [38].

Inflammation: Finally, the fourth category is the brain inflammatory diseases. We all know that the brain is protected by calvarium, dura, and blood-brain barrier (BBB) [39]. The cerebral tissue is relatively resistant to invading infections. Nevertheless, the brain or spinal cord can be inflamed, leading to swelling and irritation of tissues or vessels. The inflammatory diseases include abscess [40], meningitis [41], encephalitis [42], and vasculitis [43]. Inflammatory control [43] is first used to prevent inflammation-induced organ destruction. Then, some medications are prescribed for symptom control [44]. Finally, side-effect control is necessary since the treatments may bring in uncomfortable side effects.

Figure 3 illustrates pictures of some typical brain diseases. Figure 3(a) is a healthy brain. Figures 3(b)–(f) show several brain tumor samples. Figures 3(g)–(k) show neurodegenerative diseases. Figures 3(l)–(t) show cerebrovascular diseases. Figures 3(u)–(z) show inflammatory brains. All the images were downloaded from the "The Whole Brain Atlas".

3. MRI

Magnetic resonance imaging (MRI) uses both magnetic field and pulses, in order to generate pictures of brain anatomy. Different tissues make direct contrasts, due to their different relaxation properties [45] of the hydrogen atoms therein.

MRI is safe and painless. It does not involve radiation. Nevertheless, patients with heart pacemakers [46], cochlear implants [47], metal implants [48, 49] cannot be scanned, because of the extremely high strength magnets. This is called projectile (or missile) effect [50], referring to the dangerous ability of MRI scanner to attract ferromagnetic iron-based materials. The powerful magnet can also erase information from storage devices, such as ID badges, cell phones, subway cards, credit cards, flash drives, etc.

3.1. Shimming

Shimming is to correct the inhomogeneity of magnetic field produced by the main magnet [51]. The inhomogeneity may arise from both the imperfect of magnet and the presence of external objects (such as brain) [52]. In active shimming, currents directed through dedicated coils are used to improve homogeneity [53]. In passive shimming, small pieces of sheet metal are inserted within the scanner bore [54]. Active shim coils can be either superconducting or resistive [55]. Both active and passive shimmings are controlled by specialized circuitry and need their own power supply.

3.2. Water and Fat Suppression

Hydrogen atoms can generate a detectable radiofrequency (RF) signal, and they are abundant in both water and fat in human body. To balance the image contrast, water suppression [56] and fat suppression [57, 58] are necessary in some particular MRI scans.

Water suppression can be implemented by presaturation [59], flip-back [60], and "jump and return" [61]. Fat suppression is based on that hydrogen nuclei in fat tissues have different values for MRI-related parameters [62]. Two types of fat suppression techniques exist: (i) Relaxation dependent technique, such as short T1inversion recovery (STIR) [63]; (ii) Chemical shift-dependent techniques, including Dixon [64], water selective excitation [65], spectral fat saturation [66], and spectrally adiabatic inversion recovery (SPAIR) [67]. The comparisons of above fat suppression methods are listed in Table 3.

3.3. Other Modalities

Figures 4(a)–(c) show the MR slices in coronal, axial, and sagittal directions, respectively. In addition, three advanced imaging modalities are introduced below:

Table 3. Comparison of fat suppression techniques.

Technique	Advantage	Disadvantage
STIR	Insensitive to B_0 inhomogeneity	Increased minimal TR and total measurement time; Tissue contrast affected
Dixon	Insensitive to B_0 and B_1 inhomogeneity	Minimal TR increased
Water selective excitation	Insensitive to B_1 inhomogeneity	Increased min TE, TR and total measurement time
spectral fat saturation	Shorter TR; Tissue contrast preserved	Sensitive to B_0 and B_1 inhomogeneity
SPAIR	Insensitive to B_1 inhomogeneity; Tissue contrast preserved	Increased minimal TR

(B_0 = A constant and homogeneous magnetic field to polarize spins; B_1 = An RF magnetic field perpendicular to B_0; TE = echo time; TR = repetition time)

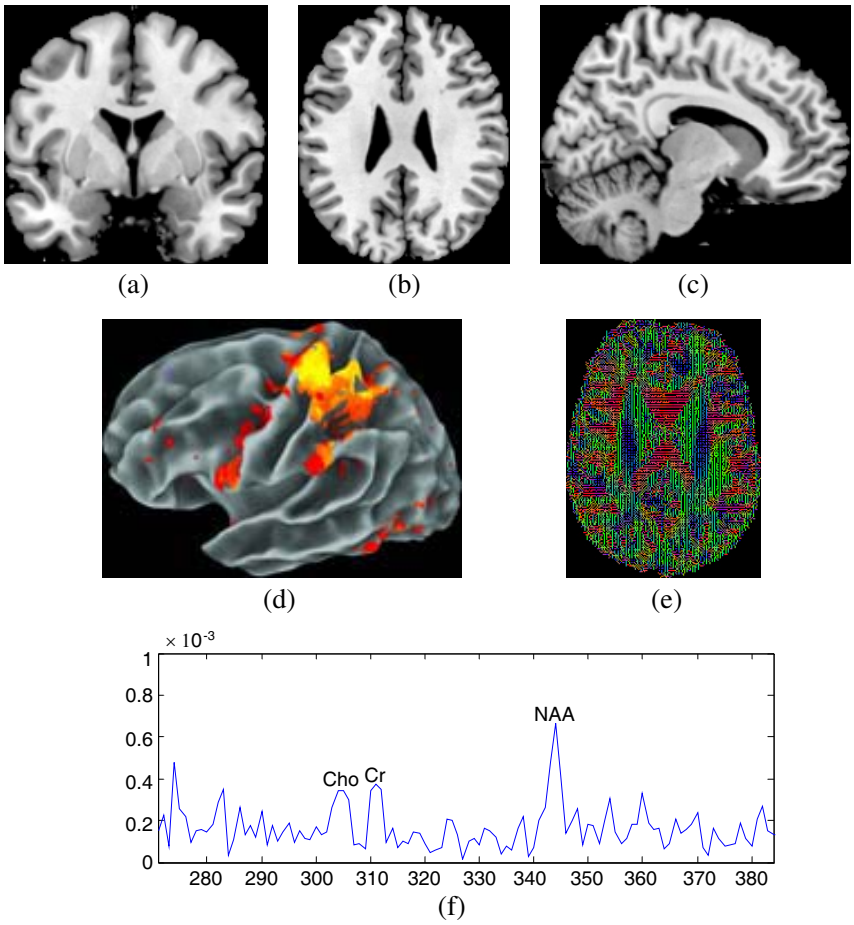

Figure 4. Illustration of MRI scans. (a) Coronal. (b) Axial. (c) Sagittal. (d) fMRI. (e) DTI. (f) Metabolic peaks at one voxel in MRSI.

fMRI: Functional MRI (fMRI) is used to measure the brain activity [68], which responds to either external stimuli or passive activity in a resting stage, as shown in Figure 4(d). It is based on the blood oxygen level dependent (BOLD) contrast [69], by imaging the changes in blood flow related to energy used by cells in the brain [70].

DTI: Diffusion tensor imaging (DTI) is another advanced neuroimaging technique, which measures the diffusion of water molecules within the brain [71], so as to produce neural tract images [72]. Each voxel in DTI is calculated from a vector or matrix from more than six different diffusion weighted acquisitions (See Figure 4(e)). The fiber directions are calculated from DTI datausing particular algorithms [73].

MRSI: Magnetic resonance spectroscopic imaging (MRSI) measures the levels of different metabolites (See Figure 4(f)) in any position within the brain [74]. Two simpler techniques are single voxel spectroscopy (SVS) [75] and chemical shift imaging (CSI) [76].

Clinically, MRSI can detect metabolic changes in strokes [77], autism [78], brain tumors [79], multiple sclerosis [80], seizure [81], depression [82], Parkinson's disease [83], Kimura disease [84], etc. Table 4 lists the identifiable metabolites (N-acetyl aspartate, choline, creatine, lipid, lactate, myo-inositol, glutamate and glutamine), and gives their peak positions and indications of change. The peaks are measures in parts per million (ppm). Note that the lipid spectrum is easily contaminated, because of the fat located in the scalp and underneath the skull.

Table 4. Metabolites with unique characteristics in MRSI.

Metabolite	Position	Indications
N-acetyl Aspartate	Major peak at 2.02 ppm	Its decrease suggests loss or damage to neuronal tissue
choline	Major peak at 3.2 ppm	Its increase suggests an increase in membrane breakdown or cell production
creatine	Major peak at 3.0 ppm	Its decrease may suggest tissue death or major cell death. Its increase could be from cranialcerebral trauma.
lipid	Major aliphatic peaks in 0.9–1.5 ppm	Its increase suggests necrosis.
lactate	A doublet at 1.33 ppm	Its presence suggests glycolysis in an oxygen deficient environment, which may arise from ischemia, hypoxia, mitochondrial disorders, and tumors.
myo-inositol	Major peak at 3.56 ppm	Its increase suggests AD, dementia, and HIV.
Glutamate & Glutamine	Resonance peaks in 2.2–2.4 ppm	Its increase may suggest hyperammonemia or hepatic encephalopathy.

4. IMAGE FEATURES

4.1. Image Preprocessing

Image Denoising: Some advanced image denoising methods have been proposed and applied to remove Rician noises and increase signal-to-noise ratio (SNR) in brain MR images [85]. The denoising algorithms should be edge preserving [86] and cannot blur important lesion information. [87] used an enhanced non-local means (NLM) algorithm. [88] explored the image space for each patch using rough set theory (RST). [89] proposed a pre-smoothing NLM filter. [90] used RST based bilateral filter (BF) to denoise brain images. [91] also used BF to eliminate noises. Parameters of BF are optimized by genetic algorithm (GA).

Slice Selection: In PBD systems, each voxel in a volumetric image can be regarded as a feature. Therefore, the slice selection is used to select where the lesion or abnormal evidence is located.

Slice selection was carried out either by neuroradiologists [92], or by hardware encoding [93], or by algorithms [94]. Note that the slice selection is not necessary, since powerful computers are becoming cheaper than ever before.

Brain Extraction: Next, it is necessary to remove the extra non-brain tissues (such as fat, skin, muscle, neck, tongue, aponeurosis, meninges, periosteum, pharynx, eye balls, etc.) from an MR image of the whole head, since they are obstacles for automatic analysis [95]. Those non-brain tissues may decrease the detection performance of brain diseases.

Skull stripping methods were developed to solve this problem. [96] presented the brain extraction tool (BET) in the FMRIB software library (FSL). [97] proposed a study-specific template selection strategy. [98] developed a multispectral adaptive region growing algorithm for axial brain extraction. [99] introduced concepts from artificial life, in order to govern a mass of deformable models. Its method had the least Hausdorff distance error with slightly less brain voxel. [100] proposed a robust skull stripping method on the basis of two irrational masks with sizes of 3×3 and 5×5, respectively. [101] developed a deep MRI brain extraction tool via 3D convolutional neural network (CNN). [102] used linear combination of discrete Gaussians (LCDG) and Markov-Gibbs random field (MGRF) models to develop an infant brain extraction tool.

Spatial Normalization: Afterwards, spatial normalization (i.e., spatial registration) is carried out, which reshapes a given brain image to a template image (i.e., reference image) [103]. Two steps are included: (i) estimation of warp field and (ii) application of warp field with resampling [104].

Usually the brain images are normalized to Montreal neurological institute (MNI) space. The FMRIB's linear image registration tool (FLIRT) [105] and FMRIB's nonlinear image registration tool (FNIRT) are excellent software that can accomplish this goal. The image processing toolbox in Matlab provides registration functions such as "imregister", "imregtform", "imregdemons", etc.

Scholars have developed more advanced spatial normalization methods: [106] proposed anatomical global spatial normalization methods, in order to scale high-resolution brains to control, without altering mean sizes of the brain structure. [107] introduced specialized templates, which applied normalization algorithms to stroke-aged subjects. [108] introduced an online spatial normalization method for real-time fMRI. [109] proposed a multistage for implementing normalization.

Intensity Normalization: Intensity normalization was used to match MR image intensities between MRI scans, so as to improve image compatibility and facilitate comparability. Table 5 shows five classical intensity normalization methods: intensity scaling [110], histogram stretching [111], histogram equalization [112], histogram normalization [113], Gaussian kernel normalization [113].

Table 5. Five intensity normalization methods.

Method	Equation
Intensity scaling	$g(x,y) = \frac{f(x,y)-f_{hl}}{f_{hh}-f_{hl}}$
Histogram stretching	$g(x,y) = \frac{f(x,y)-f_{\min}}{f_{\max}-f_{\min}}$
Histogram equalization	$g(x,y) = C(f(x,y)) \times (f_{\max} - f_{\min}) + f_{\min}$
Histogram normalization	$g(x,y) = \frac{f_{hh}-f_{hl}}{f_{\max}-f_{\min}} \times (f(x,y) - f_{\min}) + f_{hl}$
Gaussian kernel normalization	$g(x,y) = \frac{f(x,y)-m_f}{\sigma_f}$

(f represents the original image, g the intensity normalized image, f_{hh} the mean value of homogeneous high intensity ROI, f_{hl} the mean value of homogeneous low intensity ROI, $f_{\min}$ the minimum grayscale value, $f_{\max}$ the maximum grayscale value, C the normalized cumulative histogram, m_f the mean of original image, and σ_f the stand deviation of original image)

4.2. Feature Representation

Computer scientists extract shape, moment, wavelet, statistics, entropy, GLCM, and Fourier features. Table 6 shows the common features used in brain images.

Table 6. Brain image features.

Type	Variants
Shape	perimeter [114], area [115], eccentricity [116], distance [117], diameter [118], orientation [119], length [120], thickness [121],
Moment	central moment [122], Hu moment [123], Zernike moment [124], pseudo Zernike moment [125], statistical moment [126],
Wavelet	discrete wavelet transform [127], stationary wavelet transform [128], Legendre wavelet transform (LWT, also called spherical wavelet transform) [129], discrete wavelet packet transform [130], Gabor wavelet transform [131]; dual-tree complex wavelet transform [132], wavelet-space correlation [133],
Statistics	mean [134], variance [135], skewness [136], kurtosis [137], uniformity [138],
Entropy	Shannon entropy [139], wavelet entropy [140], Tsallis entropy [141], Renyi entropy [142], multiscale entropy [143], permutation entropy [144], mutual information [145], relative wavelet entropy [146],
GLCM	**Matlab generated features** (contrast, correlation, energy, homogeneity) [147], **R generated features** (mean, variance, homogeneity, contrast, dissimilarity, entropy, second moment, correlation) [148], **Haralick features** (angular second moment, contrast, correlation, sum of squared variances, inverse difference moment, sum average, sum variance, sum entropy, entropy, difference variance, difference entropy, Information measures of correlation 1 & 2, and maximal correlation coefficient) [149],
Fourier	Fourier transform [150], fractional Fourier transform [151], Taylor-Fourier transform [152], fast Fourier transform [153], non-uniform fast Fourier transform [152], sine transform [154], cosine transform [155],

Shape: The shape features are extracted over the lobes (frontal lobe, parietal lobe, occipital lobe, temporal lobe, and limbic lobe), brain stem (medullar, pons, and midbrain) [156], diencephalon [157], cerebellum [158], ventricles (lateral ventricles, third ventricle, fourth ventricle), tracts [159], vessels (artery and vein) [160], and even the whole brain.

Moment: The image moment is a weighted average of gray intensities of image pixels [161]. Supposing that I represents the image, the raw moments M are defined as

$$M_{i,j} = \sum_x \sum_y x^i y^j I(x,y) \tag{1}$$

where x and y denote the spatial coordinates. The central moments μ are defined as

$$\mu_{i,j} = \sum_x \sum_y (x-\mu_x)^i (y-\mu_y)^j I(x,y) \tag{2}$$

The central moments are translation invariant [162]. Scale invariants can be obtained by

$$\eta_{i,j} = \frac{\mu_{i,j}}{\mu_{0,0}^{\left(1+\frac{i+j}{2}\right)}} \tag{3}$$

More advanced image moments are offered. For example, Hu moments [163] are rotation invariant. Zernike moments [164] are defined over the unit circle as

$$Z_{i,j} = \frac{i+1}{\pi} \sum_x \sum_y V_{i,j}^*(x,y) I(x,y) \tag{4}$$

where $x^2 + y^2 \leq 1$, $0 \leq j \leq i$, $i - 1$ is even. V is called the Zernike polynomial of degree i and angular dependence j.

Wavelet: The wavelet features are based on the discrete wavelet transform (DWT) [165] and its variants. DWT of a signal s is calculated by passing through low-pass filter l and high-pass filter h as:

$$L = (s * l) \downarrow 2 \tag{5}$$

$$H = (s * h) \downarrow 2 \tag{6}$$

where L and H represent the low- and high-pass coefficients; $*$ is the convolution operator; $\downarrow$ is the subsampling operator. For a brain image, the DWT can be carried out along x-axis and y-axis in sequence.

Variants of DWT were proposed. For example, the stationary wavelet transform (SWT) overcame the lack of the translation-invariance of DWT [166]. The dual-tree complex wavelet transform (DTCWT) extended the real-value to complex-value and used two decomposition trees [167]. Discrete wavelet packet transform (DWPT) decomposed detail subbands at each level to create a full decomposition tree [168]. The most disadvantage of wavelet features is how to select the optimal wavelet family and how to determine the optimal decomposition level.

Statistics: The statistical measures are based on spatial pixels. Suppose the pixels $\{x\}$ as the possible values of a discrete random variable X associated with a particular probability distribution P, then we can define common statistical measures including mean, variance, standard deviation, median, skewness, and kurtosis. Table 7 shows the formula and physical meanings of those measures.

Table 7. Statistical measures.

Measure	Formula	Meaning
mean	$\mu = \mathrm{E}(x)$	expectation of central tendency
variance	$V = \mathrm{E}\left[(x-\mu)^2\right]$	expectation of squared deviation from the mean
standard deviation	$\sigma = \sqrt{\mathrm{E}\left[(x-\mu)^2\right]}$	variation of the dataset
median	$m:\ P(x \leq m) = P(x \geq m) = \frac{1}{2}$	The value separating the higher half from the lower half
skewness	$\mathrm{E}\left(\frac{x-\mu}{\sigma}\right)^3$	asymmetry of probability function from the mean
kurtosis	$\frac{\mathrm{E}\left[(x-\mu)^4\right]}{\left\{\mathrm{E}\left[(x-\mu)^2\right]\right\}^2}$	tailedness of the probability function

(E represents the expected value operator)

Entropy: The entropy is originally a statistical measure for thermodynamics, and now it has been extended to "Shannon entropy" in information theory [169]. In this context, it measures the unpredictability of information contents. The symbols are defined the same as those in statistics, and the Shannon entropy H is defined as

$$H(X) = \mathrm{E}\left[-\log_b(P(X))\right] = -\sum_i P(x_i)\log_b P(x_i) \tag{7}$$

here the unit of entropy is bit, nat, and hartley [170] for $b = 2$, e, and 10, respectively.

Scholars have proposed variants of entropy. The Renyi entropy [171] of order α is defined as

$$H_\alpha(X) = \frac{1}{1-\alpha}\log\left(\sum_i P^\alpha(x_i)\right) \tag{8}$$

where H_α represents the Renyi entropy, with $\alpha \geq 0$ and $\alpha \neq 1$ [172]. The limiting value of H_α as $\alpha \to 1$ is the Shannon entropy.

Tsallis entropy is more suitable than Shannon entropy in non-extensive system and long-range interactions [173]. Tsallis entropy is defined as

$$H_T(X) = \frac{1}{q-1}\left(1 - \sum_i p^q(x_i)\right) \tag{9}$$

where q is the entropic index. In the limit as $q \to 1$, the Tsallis entropy converts to Shannon entropy [174].

GLCM: Gray-level co-occurrence matrix (GLCM) is defined to be distribution of co-occurring values at a given offset over a brain image [175]. Supposing that the image is represented as I, the offset is $(\Delta x, \Delta y)$, then the GLCM of the image is defined as

$$G_{\Delta x,\Delta y}(i,j) = \sum_x \sum_y \begin{cases} 1 & \text{if } I(x,y) = i \& I(x+\Delta x, y+\Delta y) = j \\ 0 & \text{otherwise} \end{cases} \tag{10}$$

where G is the co-occurrence matrix, and i and j are the image intensity values. The offset makes GLCM sensitive to rotation [176], hence, the offsets in practice are chosen as 0, 45, 90, and 135 degrees at the same distance to achieve rotational invariance [177].

Three famous implementation methods are offered: (i) On the basis of Matlab platform, we can use the command "graycomatrix" to create GLCM from an image and use "graycoprops" to extract four properties as: contrast, correlation, energy, and homogeneity from the GLCM [178]. (ii) In R language, the "glcm" package [148] can obtain nine features as mean, variance, homogeneity, contrast, dissimilarity, entropy, second moment, and correlation. (iii) [179] presented total fourteen statistics with the intent of describing the texture of the image.

Fourier: Fourier transform (FT) decomposes a signal into the frequencies that make it up. For brain images, discrete Fourier transform (DFT) is normally used and converts the image into a finite combination of complex sinusoids order by frequencies. Supposing that signal X is composed of N complex numbers of $[x_0, x_1, \ldots, x_{N-1}]$, the DFT is defined as

$$\text{DFT}: \ X_k = \sum_{n=0}^{N-1} x_n \times \exp\left(-\frac{2\pi i k n}{N}\right) \tag{11}$$

The fast Fourier transform (FFT) reduces the computing complexity in DFT of $O(N^2)$ to $O(N \log N)$ [180].

In some conditions, sines and cosines are used to replace complex numbers, yielding the discrete sine transform (DST) and discrete cosine transform (DCT) with formulations below:

$$\text{DST}: \ X_k = \sum_{n=0}^{N-1} x_n \times \sin\left[\frac{\pi}{N+1}(n+1)(k+1)\right] \tag{12}$$

$$\text{DCT}: \ X_k = \sum_{n=0}^{N-1} x_n \times \cos\left[\frac{\pi}{N}\left(n+\frac{1}{2}\right)k\right] \tag{13}$$

Fractional Fourier transform (FRFT) [151] introduces a new angle parameter α, which represents the rotational angle in the time-frequency domain. The α-angle transformation of signal $x(t)$ is:

$$X_\alpha(u) = \int_{-\infty}^{\infty} K_\alpha(t,u) x(t) dt \tag{14}$$

where u represents the frequency and K the FRFT transformation kernel as

$$K_\alpha(t,u) = \sqrt{1 - i\cot\alpha} \times \exp\left(i\pi\left(t^2 \cot\alpha - 2ut\csc\alpha + u^2\cot\alpha\right)\right) \tag{15}$$

where i is the imaginary unit. The three discrete versions of FRFT include weighted-type [181], sampling type [182], and eigendecomposition type [183].

4.3. Dimension Reduction

The feature number may be too large, so dimensionality reduction (DR) is necessary to reduce the feature number. We divide DR into two categories: feature selection and feature reduction.

Feature Selection: Feature selection is aimed to find a subset of original features. Three types of feature selection methods exist based on how the selection algorithm and the model building are combined. Figure 5 shows the three types: (i) The filter methods [184] analyze the intrinsic properties

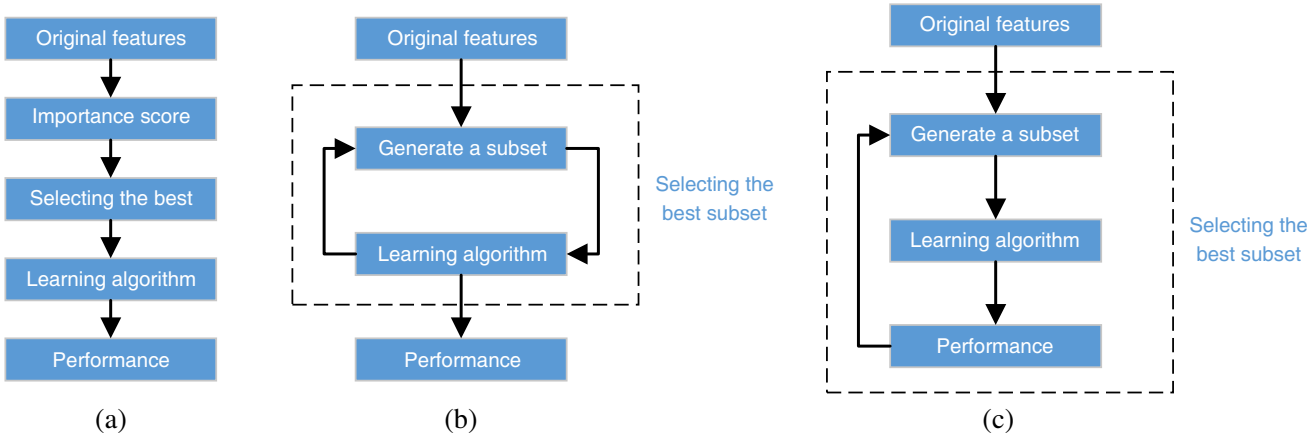

Figure 5. Three types of feature selection. (a) Filter. (b) Wrapper. (c) Embedded.

of the features, while neglecting the classifier. They first evaluate each individual feature, ignoring their interactions. Then, they rank the individual features and choose a subset. (ii) The wrapper methods [185] evaluate subsets of features and detect their potential interactions. While the number of observations is insufficient, the risk of overfitting increases. (iii) The embedded methods [186] combine the advantages of both filters and wrappers. The learning algorithms take full use of the selection algorithm, hence, their disadvantage is to determine the selection criterion and search algorithm beforehand. Table 8 lists their advantages and disadvantages.

Table 8. Comparison of feature selection methods.

Type	Advantages	Disadvantages
Filter	fast execution; robust to overfitting	may select redundant variables
Wrapper	high accuracy	slow execution; overfitting
Embedded	combination of filters and wrappers	know preliminary the selection procedure

Feature Extraction: Feature extraction transforms original features into a reduced set of features. The transformation can be either linear or nonlinear. The main linear technique is principal component analysis (PCA) [187], which maps original features to low-dimensional space in the way that the variance of transformed feature is maximized [188]. [189] is an extension of PCA, and it is capable of constructing nonlinear mappings.

Some nonlinear methods can be viewed as defining a graph-based kernel for PCA. Those methods include Laplacian eigenmap [190], Isomap [191], locally linear embedding (LLE) [192], etc. These techniques generate a low-dimensional transformed feature via a cost function and retains the local properties of original feature.

Semidefinite embedding (SDE) [193] learns the kernel using semidefinite programming instead of using fixed kernels. It first creates a neighborhood graph, where each input feature is connected with its k-nearest input features, and all k-nearest neighbors are fully connected with each other. Next, the semidefinite programming [194] aims to find an inner product matrix that maximizes the pairwise distances between any two inputs that are not connected.

Autoencoder is a feed-forward non-recurrent neural network to learn a representation for a set of features [195]. The output layer of autoencoder has the same number of nodes as in the input layer [196]. Instead of being trained to target value in the traditional neural network, autoencoder is trained to reconstruct its own input features [197]. Therefore, autoencoders can be used for dimensionality reduction.

5. CLASSIFIERS

In the classification stage, the supervised learning (SL) techniques are commonly employed. Each observation is labeled (i.e., associated with a target value), and the pair is submitted into the classifier.

5.1. Predesign

Five major points need to be predesigned before training:

(1) Dimensionality reduction: The brain scanners always acquire more redundant features than needed, which confuses the learning algorithm. We need to use the "dimensionality reduction (DR)" techniques mentioned in Section 4.3 to remove redundant features, so as to improve the classification performance.

(2) Tradeoff between bias and variance: The classification performance is related to both bias and variance [198] of the learning algorithm over several given datasets. A learning algorithm with low bias should be versatile to other datasets [199]. Hence, a good learning algorithm should balance the bias and variance automatically.

(3) Data amount and classifier complexity: If the classifier is complicated, then it is learnable from an exceptionally large dataset with low bias and high variance. In contrast, a simple classifier is learnable from a small training data with high bias and low variance. Therefore, the learning algorithm should adjust itself, taking into consideration of both the data amount and structural complexity [200].

(4) Class-imbalance problem: It is easy to obtain brain images from healthy controls, but it is quite difficult to acquire MR images from patients, particularly those disobedient patients. A medical diagnosis dataset often contains rarely positive observations and numerous negative ones [201]. This will lead to low sensitivity and high specificity. Several techniques can be used to alleviate the class imbalance problem, such as resampling [202], cost-sensitive boosting [203], cost sensitive learning [204], ensemble [205], etc.

(5) Noises in targets: The targets may be incorrect, since neuroradiologists may mislabel the brain images. This gives us a suggestion that the learning algorithm does not need to exactly match the training data [206]. Those noises in targets can be modeled as deterministic noise [207] and can be alleviated by "overfitting prevention" techniques. In practice, it is necessary to detect and remove mislabeled brain images [208].

Table 9. Six learning models.

Basic Model	Extension
DT	ID3 [209], C4.5 [210], See5 [211], incremental DT [212], alternating DT [213], neuro-fuzzy DT [214],
ELM	constrained ELM [215], optimized pruning ELM [216], state preserving ELM [217], weighted ELM [218], robust ELM [219], online sequential ELM [220], cluster regularized ELM [221], kernel ELM [222],
FNN	local coupled FNN [223], partially connected FNN [224], wavelet FNN [225], hybrid double FNN [226], time-lagged FNN [227], weight initialization FNN [228],
kNN	Evidential editing kNN [229], coupled kNN [230], integrated kNN [231], adaptive kNN [232], kNN++ [233], pairwise kNN [234],
NBC	Augmented semi NBC [235], hierarchical spatio-temporal NBC [236], weighted NBC [237], tree-augmented NBC [238],
SVM	kernel SVM [239], support vector clustering [240], transductive SVM [241], least-square SVM [242], proximal SVM [243], twin SVM [244], generalized eigenvalue proximal SVM [245], fuzzy SVM [246],

5.2. Learning Models

The most widely used learning models and their extensions are listed in Table 9, including the decision tree (DT), extreme learning machine (ELM), k-nearest neighbors (kNN), naive Bayes classifier (NBC), support vector machine (SVM), and feed-forward neural network (FNN).

Besides, some mixture models are proposed, which combine more than two basic learning models, such as inclined local naive Bayes nearest neighbor [247], support vector machine decision tree [248], etc. Those mixture models try to take the advantages of both basic learning models, and thus they often perform better than individual learning model.

5.3. Kernel Methods

Kernel methods use kernel functions to map original input features into high-dimensional feature space [249]. The advantage is that it does not need to compute the feature explicitly in high-dimensional space, but rather computes the inner products among all pairs of data in original feature space [250]. Popular kernel functions are listed in Table 10.

Table 10. Five popular kernel functions.

Name	Function	Parameter
Linear	$K(x,y) = x^T y$	
Homogeneous Polynomial (HPOL)	$K(x,y) = \left(x^T y\right)^d$	$d > 0$
Inhomogeneous Polynomial (IPOL)	$K(x,y) = \left(x^T y + c\right)^d$	$c \geq 0$, $d > 0$
Radial basis function (RBF)	$K(x,y) = \exp\left(-\gamma \left\|x - y\right\|^2\right)$	γ
Sigmoid	$K(x,y) = \tanh\left(cx^T y + d\right)$	c, d

5.4. Optimization

The training of a learning model is an optimization problem. Traditional gradient descent based methods may fall into local optima, hence, global optimization methods [251] are employed for classifier training as

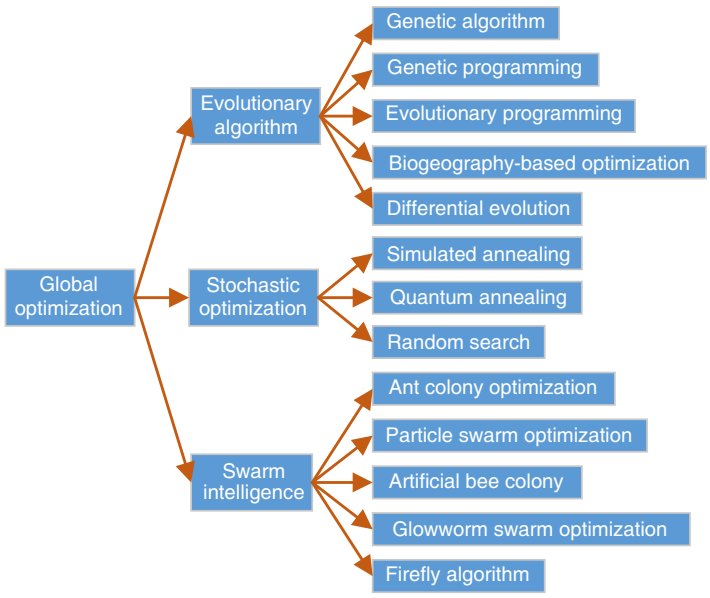

Figure 6. Global optimization algorithms.

they are aimed for finding all optimal points. Figure 6 shows three main categories of global optimization methods: evolutionary algorithm (EA), Stochastic optimization (SO), and swarm intelligence (SI).

Evolutionary algorithm: EA uses mechanism inspired by biological evolution [252]. It uses reproduction, mutation, recombination, selection, and other evolution-related operators [253]. The candidates for solutions are individuals in a population and are measured by fitness function.

The population evolution occurs every iteration in the way that the candidates get closer to the global optimal point. EA includes genetic algorithm (GA) [254], differential evolution (DE) [255], genetic programming [256], evolutionary strategy, etc. The biogeography-based optimization (BBO) method [257] is a new EA method that mimics the evolution of distribution of biological species along time and space [258, 259].

Stochastic optimization: SO uses random variables with random iterates to accelerate search [260]. It can solve both stochastic optimization problems and deterministic optimization problems. The injected randomness can guarantee the search less sensitive to modeling errors and escape from local minima points [261]. The common SO methods include simulated annealing (SA) [262], quantum annealing (QA) [263], random search, etc.

Swarm intelligence: SI investigates the collective behavior of decentralized and self-organized systems [264]. Narrowly speaking, SI refers to a series of optimization algorithms that mimics the nature SI systems: bacterial growth, fish schooling, ant colony, bird flocking, and animal herding. The two famous SI algorithms are ant colony optimization (ACO) [265] and particle swarm optimization (PSO) [266]. Other popular SI algorithms include artificial bee colony (ABC) [267], firefly algorithm (FA) [268], and glowworm swarm optimization.

6. CURRENT PBD SYSTEMS

6.1. Benchmark

Commonly used datasets can be downloaded from the homepage of "the whole brain atlas" from Harvard Medical School. No more than five slices are selected from each subject (pathological or healthy). The slices selected from patients should cover the lesions by confirmation of three radiologists with over ten years of experiences. The slices from healthy subjects are selected at random from the same range of patient slices.

Three benchmark datasets (DI, DII, and DIII) are generated based on collection of above images. The former two datasets (DI& DII) contain seven types of diseases. DI consists of 66 images, and DII consists of 160 images. The largest dataset DIII contains 11 types of diseases and 255 images. Note that the images in the Harvard Medical School website are mainly for didactic use, and it only collects those patients with prominent abnormal features from healthy brains. Hence, the performance over the datasets only reflects the algorithm performance in ideal conditions and cannot reflect the algorithm performance in real-world scenario where the scanned images are usually of poor quality.

6.2. Statistical Analysis

K-fold stratified cross validation (SCV) is commonly used. Compared to standard cross validation, the stratification rearranges the data so that each fold is a full representative of the whole dataset. Usually, three benchmark datasets are divided in the way of Table 11. To further reduce the randomness, we

Table 11. SCV setting.

Dataset	K	Training		Validation		Total	
		H	P	H	P	H	P
DI	6	15	40	3	8	18	48
DII	5	16	112	4	28	20	140
DIII	5	28	176	7	44	35	220

(K represents the number of fold, H = Healthy, P = Pathological)

Table 12. Comparison of state-of-the-art PBD systems.

Approach	Feature	DR	F.N.	Classifier	Opt. Met.	R.N.	DI	DII	DIII
[269]	DWT		4761	SOM		5	94.00	93.17	91.65
	DWT		4761	SVM		5	96.15	95.38	94.05
	DWT		4761	SVM + IPOL		5	98.00	97.15	96.37
	DWT		4761	SVM + RBF		5	98.00	97.33	96.18
[270]	DWT	PCA	7	FNN		5	97.00	96.98	95.29
	DWT	PCA	7	kNN		5	98.00	97.54	96.79
[271]	DWT	PCA	19	FNN	SCG	5	100.00	99.27	98.82
[272]	DWT	PCA	19	SVM		5	96.01	95.00	94.29
	DWT	PCA	19	SVM + RBF		5	100.00	99.38	98.82
[273]	WE	SWP	3	PNN		5	100.00	99.88	98.90
[274]	RT	PCA	9	LS-SVM		5	100.00	100.00	99.39
[275]	DWTE		16	GEPSVM		10	100.00	100.00	99.33
	DWTE		16	GEPSVM + RBF		10	100.00	100.00	99.53
[276]	WE		7	NBC		10	92.58	91.87	90.51
[277]	SWT	PCA	7	FNN	IABAP	10	100.00	99.44	99.18
	SWT	PCA	7	FNN	ABC-SPSO	10	100.00	99.75	99.02
	SWT	PCA	7	FNN	HPA	10	100.00	100.00	99.45
[278]	WE		6	FNN	HBP	10	100.00	100.00	99.49
[279]	WE + HMI		14	GEPSVM		10	100.00	99.56	98.63
	WE + HMI		14	GEPSVM + RBF		10	100.00	100.00	99.45
[280]	SWT	PCA	7	GEPSVM		10	100.00	99.62	99.02
	SWT	PCA	7	GEPSVM + RBF		10	100.00	100.00	99.41
[281]	WPSE		16	SVM		10	98.64	97.12	97.02
	WPTE		16	SVM		10	99.09	98.94	98.39
	WPSE		16	FSVM		10	99.85	99.69	98.94
	WPTE		16	FSVM		10	100.00	100.00	99.49
[282]	FRFE	WTT	12	NBC		10	97.12	95.94	95.69
	FRFE	WTT	12	SVM		10	100.00	99.69	98.98
	FRFE	WTT	12	GEPSVM		10	100.00	100.00	99.18
	FRFE	WTT	12	TSVM		10	100.00	100.00	99.57
[165]	DWT	PPCA	13	ADBRF		5	100.00	99.30	98.44
	DWT	PPCA	13	ADBRF		5	100.00	100.00	99.53
[283]	SWE		6	FNN	HBP	10	100.00	100.00	99.53
[284]	SWT	PCA	7	SVM + HPOL		10	100.00	99.56	98.51
	SWT	PCA	7	SVM + IPOL		10	100.00	99.69	98.55
	SWT	PCA	7	SVM + RBF		10	100.00	99.69	99.06
[285]	DTCWT	VE	12	SVM		10	100.00	99.69	98.43
	DTCWT	VE	12	GEPSVM		10	100.00	99.75	99.25
	DTCWT	VE	12	TSVM		10	100.00	100.00	99.57
[286]	WE		2	PNN	BPSO-MT	10	100.00	100.00	99.53
[287]	FRFE		12	MLP	ARCBBO	10	99.85	98.38	97.02
	FRFE		12	DP-MLP	ARCBBO	10	100.00	99.19	98.24
	FRFE		12	BDB-MLP	ARCBBO	10	100.00	99.31	98.12
	FRFE		12	KC-MLP	ARCBBO	10	100.00	99.75	99.53

(All methods here are of Type 1, i.e., for all brain diseases detection)

tend to run the K-fold SCV more than once. Traditionally, the K-fold SCV ran five times. In recent years, a ten-time repetition can give more accurate results than a five-time repetition.

6.3. Quantitative Comparison

We compare 44 state-of-the-art PBD systems in this survey and present the results in Table 12. The first column lists the author and year. The second column lists the names of employed features. The third column lists the dimension reduction (DR) technique. The four column lists the number of features submitted to classifier. The fifth column lists the classifier model. The sixth column presents the optimization method. The seventh column presents the run times. The final three columns show the accuracy over three benchmark datasets. To save the space, the names of all algorithms are abbreviated, and the full meanings can be found in Table A1.

From Table 12, we can observe that all 44 approaches follow the scheme described in this survey. Besides, the DI dataset is too small, so that nearly all algorithms achieve exact detection. The DII dataset contains 160 brain images of 7 diseases, and several algorithms achieve perfect classification. The largest DIII dataset contains 255 brain images with 11 diseases, and no algorithm can detect the pathological brains perfectly. The best algorithms for DIII till now are FRFT + WTT + TSVM [282] and DTCWT + VE + TSVM [285] with a detection accuracy of 99.57%.

6.4. Future Researches

In the hospitals, we have a small number of labeled brain images and a large number of unlabeled brain images. When creating the PBD systems, we usually discard the unlabeled brain images and merely make use of the labeled brain images. Nevertheless, scholars have found unlabeled data used with labeled data can produce significant improvement [288]. The semi-supervised learning (SSL) is a mixture of unsupervised learning and supervised learning [289]. It can make full use of both labeled data and unlabeled data [290]. Therefore, the SSL technique may be practical in PBD situations.

In another situation, we may have some successful detection systems (such as an AD detection system) before developing a PBD system. Can the AD detection system help us generate the PBD system? This can be answered by the "transfer learning" technique [291, 292], which is based on the idea that it would be easier to learn to speak Japanese having already learned to speak Chinese. Transfer learning can apply the knowledge gained while developing the AD detection system, to the related problem of generating a PBD system.

The AI techniques in MR images can also be applied to computed tomography (CT) [293, 294], positron emission tomography (PET), single-photon emission computerized tomography (SPECT), confocal laser scanning microscopy (CLSM) [295], etc. Besides, advanced optimization may augment the classification performance. We will test the adaptive chaotic PSO [296], water drop algorithm [297], bacterial chemotaxis optimization (BCO) [298], grey wolf optimization [299], social spider optimization [300], etc.

In all, this survey gives the latest AI techniques in PBD systems and offers a quantitative comparison. We expect that the readers are awakened with intense interest in this field.

APPENDIX A.

Table A1. Acronym list.

Acronym	Definition
3D	three dimensional
ABC	artificial bee colony
ABC-SPSO	ABC with Standard PSO
ACO	ant colony optimization
AD	Alzheimer's disease

ADBRF	AdaBoost with random forest
AI	artificial intelligence
AIDS	acquired immune deficiency syndrome
ARCBBO	adaptive real-coded BBO
BBB	blood-brain barrier
BBO	biogeography-based optimization
BCO	bacterial chemotaxis optimization
BDB	Bayesian detection boundary
BET	brain extraction tool
BF	bilateral filter
BOLD	blood oxygen level dependent
BPSO-MT	binary PSO with mutation and TVAC
CAD	computer-aided diagnosis
CBF	cerebral blood flow
CLSM	confocal laser scanning microscopy
CNN	convolutional neural network
CSI	chemical shift imaging
CT	computed tomography (CT)
DCT	discrete cosine transform
DE	differential evolution
DFT	discrete Fourier transform
DP	dynamic pruning
DR	dimensionality reduction
DST	discrete sine transform
DT	decision tree
DTCWT	dual-tree complex wavelet transform
DTI	diffusion tensor imaging
DWPT	discrete wavelet packet transform
DWT	discrete wavelet transform
DWTE	discrete wavelet Tsallis entropy
EA	evolutionary algorithm
ELM	extreme learning machine
FA	firefly algorithm
FFT	fast Fourier transform
FLIRT	FMRIB's linear image registration tool
fMRI	functional MRI
FNIRT	FMRIB's nonlinear image registration tool
FNN	feed-forward neural network
FRFE	fractional Fourier entropy
FRFT	fractional Fourier transform
FSL	FMRIB software library
FSVM	fuzzy SVM
FT	Fourier transform

GA	genetic algorithm
GEPSVM	generalized eigenvalue proximal SVM
GLCM	gray-level co-occurrence matrix
GSO	glowworm swarm optimization
HBP	Hybridization of BBO and PSO
HIV	human immunodeficiency virus
HMI	Hu moment invariant
HPA	hybridization of PSO and ABC
HPOL	homogeneous polynomial
IABAP	Integrated algorithm based on ABC and PSO
ID	identification
IPOL	inhomogeneous polynomial
KC	Kappa coefficient
kNN	k-nearest neighbors
LCDG	linear combination of discrete Gaussians
LLE	locally linear embedding
LS	least square
LWT	Legendre wavelet transform
MGRF	Markov-Gibbs random field
MLP	multi-layer Perceptron
MNI	Montreal neurological institute
MR	magnetic resonance
MRI	magnetic resonance imaging
MRSI	magnetic resonance spectroscopic imaging
NBC	naive Bayes classifier
NLM	non-local means
PBD	pathological brain detection
PCA	principal component analysis
PET	positron emission tomography
PNN	probabilistic neural network
PPCA	Probabilistic PCA
ppm	parts per million
PR	pattern recognition
PSO	particle swarm optimization
QA	quantum annealing
RBF	radial basis function
ROI	region of interest
RST	rough set theory
RT	Ripplet transform
SA	simulated annealing
SAH	subarachnoid hemorrhage
SCG	scaled conjugate gradient
SCV	stratified cross validation

SDE	semidefinite embedding
SI	swarm intelligence
SL	supervised learning
SNR	signal-to-noise ratio
SO	stochastic optimization
SOM	self-organizing map
SPAIR	spectrally adiabatic inversion recovery
SPECT	single-photon emission computerized tomography
SSL	semi-supervised learning
STIR	short T1 inversion recovery
SVM	support vector machine
SVS	single voxel spectroscopy
SWE	stationary wavelet entropy
SWP	spider web plot
SWT	stationary wavelet transform
TE	echo time
TIA	transient ischemic attack
TLE	temporal lobe epilepsy
TR	repetition time
TSVM	twin SVM
TVAC	time-varying acceleration coefficient
VE	variance and entropy
WE	wavelet entropy
WPSE	wavelet packet Shannon entropy
WPTE	wavelet packet Tsallis entropy
WTT	Welch's t-test

Conflict of Interest

The authors declare that there is no conflict of interests regarding the publication of this paper.

ACKNOWLEDGMENT

This survey was supported by NSFC (61503188), Natural Science Foundation of Jiangsu Province (BK20150983), Nanjing Normal University Research Foundation for Talented Scholars (2013119XGQ0061), Open Project Program of the State Key Lab of CAD&CG (A1616), Open Fund of Key laboratory of symbolic computation and knowledge engineering of ministry of education (93K172016K17), and Open Fund of Key Laboratory of Statistical information technology and data mining (SDL201608).

REFERENCES

1. Gnecco, G., *J. Optim. Theory Appl.*, Vol. 168, 488, 2016.
2. Mori, C., et al., *Amyloid Precursor Protein: A Practical Approach*, W. Xia, et al. (eds.), 165, CRC Press-Taylor & Francis Group, 2005.
3. Wain, R. A., et al., *Symposium on Computer Applications in Medical Care*, 94, 1991.
4. Lloret, R. L., et al., *American Heart Journal*, Vol. 110, 761, 1985.
5. Cavestri, R., et al., *Minerva Medica*, Vol. 82, 815, 1991.

6. Brai, A., et al., *Computers and Biomedical Research*, Vol. 27, 351, 1994.
7. Juhola, M., et al., *Medical Informatics*, Vol. 20, 133, 1995.
8. Imran, M. B., et al., *Nuclear Medicine Communications*, Vol. 20, 25, 1999.
9. Terae, S., et al., *International Congress Series*, 459, H. U. Lemke, et al. (eds.), Elsevier Science Publishers, 1998.
10. Barra, V., et al., *JMRI — Journal of Magnetic Resonance Imaging*, Vol. 11, 267, 2000.
11. Antel, S. B., et al., *Epilepsia*, Vol. 44, 255, 2003.
12. Coulon, D., et al., *IEEE Transactions on Pattern Analysis and Machine Intelligence*, Vol. 1, 94, 1979.
13. Bartels, P. H., et al., *Acta Cytologica*, Vol. 18, 376, 1974.
14. Bonettini, S., et al., *Appl. Math. Comput.*, Vol. 286, 288, 2016.
15. Dorigo, M., Politecnico di Milano, Italy, 1992.
16. Kennedy, J., et al., *IEEE International Conference on Neural Networks*, 1942, IEEE, 1995.
17. Storn, R., et al., *Journal of Global Optimization*, Vol. 11, 341, 1997.
18. Karaboga, D., et al., *Foundations of Fuzzy Logic and Soft Computing*, P. Melin, et al. (eds.), 789, Springer-Verlag Press, Berlin, 2007.
19. Krishnanand, K. N., et al., *IEEE Swarm Intelligence Symposium*, 84, IEEE, Pasadena, 2005.
20. Gaviani, P., et al., *Neurol. Sci.*, Vol. 34, 2151, 2013.
21. Chandra, S., et al., *J. Neuro-Oncol.*, Vol. 127, 33, 2016.
22. Matsunaga, S., et al., *World Neurosurg.*, Vol. 89, 455, 2016.
23. Sands, S. A., *J. Clin. Oncol.*, Vol. 34, 1024, 2016.
24. Rathe, M., et al., *Chemotherapy*, Vol. 61, 204, 2015.
25. Martinez-Gonzalez, A., et al., *Mathematical Medicine and Biology*, Vol. 32, 239, 2015.
26. Hou, J. X., et al., *CNS Neurosci. Ther.*, Vol. 22, 244, 2016.
27. Chanda, S., et al., *Proc. Natl. Acad. Sci. U.S.A.*, Vol. 110, 16622, 2013.
28. Hanif, U., et al., *37th Annual International Conference of the IEEE Engineering in Medicine and Biology Society*, 6002, IEEE, Milan, Italy, 2015.
29. Menezes, R., et al., *Medicine*, Vol. 94, e971, 2015.
30. Srulijes, K., et al., *BMC Neurol.*, Vol. 15, 192, 2015.
31. Kulminski, A. M., et al., *Rejuv. Res.*, Vol. 18, 128, 2015.
32. Anderson, K. N., et al., *Nature and Science of Sleep*, Vol. 5, 61, 2013.
33. Martinez-Perez, B., et al., *Health Inform. J.*, Vol. 21, 267, 2015.
34. Stone, N. J., et al., *Mayo Clinic Proceedings*, Vol. 91, 692, 2016.
35. Everson-Rose, S. A., et al., *Stroke*, Vol. 45, 2318, 2014.
36. Spurgeon, L., et al., *Psychol. Health Med.*, Vol. 21, 632, 2016.
37. Yolas, C., et al., *World Neurosurg.*, Vol. 86, 79, 2016.
38. Akanuma, K., et al., *J. Clin. Neurosci.*, Vol. 28, 128, 2016.
39. Troletti, C. D., et al., *Biochim. Biophys. Acta-Mol. Basis Dis.*, Vol. 1862, 452, 2016.
40. Slone, H. W., et al., *Clin. Imaging*, Vol. 37, 361, 2013.
41. Shyu, L. Y., et al., *Zoonoses Public Health*, Vol. 61, 411, 2014.
42. Thomas, A. C., et al., *Clin. Nucl. Med.*, Vol. 40, 358, 2015.
43. Gonzalez-Suarez, I., et al., *Cerebrovasc. Dis.*, Vol. 41, 313, 2016.
44. Sadatsafavi, M., et al., *Allergy*, Vol. 71, 371, 2016.
45. Rerich, E., et al., *NMR in Biomedicine*, Vol. 28, 1402, 2015.
46. Pooley, R. A., et al., *American Journal of Roentgenology*, Vol. 206, 230, 2016.
47. Grupe, G., et al., *HNO*, Vol. 64, 156, 2016.
48. Sykora, M., et al., *Ceska a Slovenska Neurologie a Neurochirurgie*, Vol. 71, 47, 2008.

49. Mattei, E., et al., *PIERS Proceedings*, 639–642, Marrakesh, Morocco, Mar. 20–23, 2011.
50. Muhlenweg, M., et al., *Radiologe*, Vol. 55, 638, 2015.
51. Brink, W. M., et al., *Magn. Reson. Med.*, Vol. 75, 2185, 2016.
52. Schneider, R., et al., *Magn. Reson. Med.*, Vol. 74, 934, 2015.
53. Ahn, M. C., et al., *IEEE Trans. Appl. Supercond.*, Vol. 25, 4300804, 2015.
54. Kong, X., et al., *J. Magn. Reson.*, Vol. 263, 122, 2016.
55. Toth, J., et al., *IEEE Trans. Appl. Supercond.*, Vol. 23, 4300104, 2013.
56. Giraudeau, P., et al., *Metabolomics*, Vol. 11, 1041, 2015.
57. Tagliafico, A., et al., *Radiologia Medica*, Vol. 121, 45, 2016.
58. Van der Velden, T. A., et al., *Magn. Reson. Imaging*, Vol. 34, 462, 2016.
59. Goez, M., et al., *J. Magn. Reson.*, Vol. 177, 236, 2005.
60. Lippens, G., et al., *Journal of Biomolecular NMR*, Vol. 5, 327, 1995.
61. Louis-Joseph, A., et al., *Chem. Phys. Lett.*, Vol. 337, 92, 2001.
62. https://mriatmrc.com/fb/body-mri/fat-suppression-techniques/, 2013.
63. Kobayashi, T., et al., *Magn. Reson. Med. Sci.*, Vol. 13, 67, 2014.
64. Guerini, H., et al., *Semin. Musculoskelet. Radiol.*, Vol. 19, 335, 2015.
65. Deligianni, X., et al., *Magn. Reson. Med.*, Vol. 72, 800, 2014.
66. Clauser, P., et al., *Eur. Radiol.*, Vol. 24, 2213, 2014.
67. Choi, W. H., et al., *Korean Journal of Spine*, Vol. 9, 227, 2012.
68. Brier, M. R., et al., *Journal of Neurology*, Vol. 263, 1083, 2016.
69. Markuerkiaga, I., et al., *Neuroimage*, Vol. 132, 491, 2016.
70. Weerakoon, B. S., et al., *Appl. Magn. Reson.*, Vol. 47, 453, 2016.
71. Xiong, J., et al., *Eur. Radiol.*, Vol. 26, 1705, 2016.
72. Taso, M., et al., *NMR in Biomedicine*, Vol. 29, 817, 2016.
73. Chen, G. X., et al., *Sci. Rep.*, Vol. 6, 21825, 2016.
74. Sparacia, G., et al., *Neuradiology J.*, Vol. 29, 160, 2016.
75. Lee, S. J., et al., *Appl. Magn. Reson.*, Vol. 45, 1333, 2014.
76. Fuchs, J., et al., *Magn. Reson. Mat. Phys. Biol. Med.*, Vol. 28, 127, 2015.
77. Whiteley, W. N., et al., *Neurology*, Vol. 79, 152, 2012.
78. Goh, S., et al., *JAMA Psychiatry*, Vol. 71, 665, 2014.
79. Belkic, D., et al., *J. Math. Chem.*, Vol. 54, 602, 2016.
80. Fleischer, V., et al., *Mult. Scler. J.*, Vol. 20, 310, 2014.
81. O'Neill, J., et al., *Epilepsia*, Vol. 52, 1705, 2011.
82. Harper, D. G., et al., *Am. J. Geriatr. Psychiatr.*, Vol. 22, 499, 2014.
83. Ciurleo, R., et al., *Neurosci. Lett.*, Vol. 599, 55, 2015.
84. Wang, J., et al., *J. Craniofac. Surg.*, Vol. 25, 2147, 2014.
85. Shi, L. Y., et al., *Fluct. Noise Lett.*, Vol. 14, 1550002, 2015.
86. Zhang, Y., et al., *Science in China Series F: Information Sciences*, Vol. 51, 2115, 2008.
87. Iftikhar, M. A., et al., *Int. J. Imaging Syst. Technol.*, Vol. 24, 52, 2014.
88. Phophalia, A., et al., *Signal Process.*, Vol. 103, 24, 2014.
89. Yang, J., et al., *Biomed. Eng. Online*, Vol. 14, 2, 2015.
90. Phophalia, A., et al., *Appl. Soft. Comput.*, Vol. 33, 1, 2015.
91. Akar, S. A., *Appl. Soft. Comput.*, Vol. 43, 87, 2016.
92. Mirsadraee, S., et al., *Quant. Imaging Med. Surg.*, Vol. 6, 42, 2016.
93. Middione, M. J., et al., *Magn. Reson. Med.*, Vol. 71, 2014, 2014.
94. Yuan, T. F., et al., *Frontiers in Computational Neuroscience*, Vol. 9, 66, 2015.
95. Kalavathi, P., et al., *Journal of Digital Imaging*, Vol. 29, 365, 2016.

96. Smith, S. M., *Hum. Brain Mapp.*, Vol. 17, 143, 2002.
97. Doshi, J., et al., *Acad. Radiol.*, Vol. 20, 1566, 2013.
98. Roura, E., et al., *Comput. Meth. Programs Biomed.*, Vol. 113, 655, 2014.
99. Prasad, G., et al., *J. Neurosci. Methods*, Vol. 236, 114, 2014.
100. Moldovanu, S., et al., *Journal of Digital Imaging*, Vol. 28, 738, 2015.
101. Kleesiek, J., et al., *Neuroimage*, Vol. 129, 460, 2016.
102. Alansary, A., et al., *IEEE J. Biomed. Health Inform.*, Vol. 20, 925, 2016.
103. Kronfeld, A., et al., *Med. Phys.*, Vol. 42, 6875, 2015.
104. Shattuck, D. W., et al., *Neuroimage*, Vol. 39, 1064, 2008.
105. Jenkinson, M., et al., *Neuroimage*, Vol. 17, 825, 2002.
106. Lancaster, J. L., et al., *Neuroinformatics*, Vol. 8, 171, 2010.
107. Rorden, C., et al., *Neuroimage*, Vol. 61, 957, 2012.
108. Li, X. F., et al., *PLoS One*, Vol. 9, e103302, 2014.
109. Weiss, M., et al., *Brain Struct. Funct.*, Vol. 220, 1695, 2015.
110. Abbott, D. F., et al., *Neuroimage*, Vol. 44, 812, 2009.
111. Brahim, A., et al., *Appl. Soft. Comput.*, Vol. 37, 234, 2015.
112. Babu, P., et al., *Int. J. Imaging Syst. Technol.*, Vol. 25, 24, 2015.
113. Loizou, G. P., et al., *Journal of Biomedical Graphics and Computing*, Vol. 3, 20, 2013.
114. Zanier, E. R., et al., *Intensive Care Medicine Experimental*, Vol. 3, 39, 2015.
115. Green, T., et al., *Hum. Brain Mapp.*, Vol. 37, 1593, 2016.
116. Jespersen, S. N., et al., *NMR in Biomedicine*, Vol. 26, 1647, 2013.
117. Su, Z., et al., *Information Processing in Medical Imaging*, Vol. 24, 411, 2015.
118. Gutierrez, J., et al., *J. Am. Heart Assoc.*, Vol. 4, e002289, 2015.
119. Ziegel, J. F., et al., *Scand. J. Stat.*, Vol. 42, 813, 2015.
120. Taketani, K., et al., *Congenit. Anom.*, Vol. 55, 99, 2015.
121. Green, T., et al., *Am. J. Med. Genet. B*, Vol. 171, 402, 2016.
122. Santiago-Mozos, R., et al., *40th Annual Meeting on Computing in Cardiology*, 425, IEEE, Zaragoza, Spain, 2013.
123. Zaki, W., et al., *J. Electron. Imaging*, Vol. 19, 043021, 2010.
124. Thapaliya, K., et al., *Int. J. Imaging Syst. Technol.*, Vol. 24, 284, 2014.
125. Gorji, H. T., et al., *Neuroscience*, Vol. 305, 361, 2015.
126. Hsu, Y. H. H., et al., *Magn. Reson. Imaging*, Vol. 31, 618, 2013.
127. Zhang, Y., et al., *The Scientific World Journal*, 130134, 2013.
128. Bendib, M. M., et al., *Pattern Anal. Appl.*, Vol. 18, 829, 2015.
129. Nain, D., et al., *IEEE Trans. Med. Imaging*, Vol. 26, 598, 2007.
130. Perez, G., et al., *Integr. Comput.-Aided Eng.*, Vol. 21, 163, 2014.
131. Nabizadeh, N., et al., *Comput. Electr. Eng.*, Vol. 45, 286, 2015.
132. Renjith, A., et al., *Journal of Medical Engineering & Technology*, Vol. 39, 498, 2015.
133. Li, Y., et al., *Magn. Reson. Med.*, Vol. 74, 1574, 2015.
134. Lopez-Mejia, M., et al., *J. Stroke Cerebrovasc. Dis.*, Vol. 25, 515, 2016.
135. Tisdall, M. D., et al., *Neuroimage*, Vol. 127, 11, 2016.
136. Sun, Y., et al., *16th IEEE International Conference on Image Processing*, B. Gimi, et al. (eds.), 661, IEEE, Cairo, Egypt, 2009.
137. Nardone, V., et al., *Cureus*, Vol. 8, e584, 2016.
138. Song, K. H., et al., *J. Neurosci. Methods*, Vol. 255, 75, 2015.
139. Chaudhari, A. K., et al., *3rd IEEE International Advance Computing Conference*, B. M. Kalra, et al. (eds.), 1229, IEEE, Ghaziabad, India, 2013.

140. Bhagat, M., et al., *PLoS One*, Vol. 4, e7173, 2009.
141. Wu, L., *Sensors*, Vol. 8, 7518, 2008.
142. Gao, J. H., et al., *PLoS One*, Vol. 6, e24446, 2011.
143. Escudero, J., et al., *Brain Res. Bull.*, Vol. 119, 136, 2015.
144. Ferlazzo, E., et al., *Clin. Neurophysiol.*, Vol. 125, 13, 2014.
145. Wang, X. X., et al., *Medical Imaging 2015: Biomedical Applications in Molecular, Structural, and Functional Imaging*, B. Gimi, et al. (eds.), 94171N, SPIE-Int. Soc. Optical Engineering, Bellingham, 2015.
146. Frantzidis, C. A., et al., *Front. Aging Neurosci.*, Vol. 6, 224, 2014.
147. Singh, D., et al., *International Journal of Engineering and Advanced Technology*, Vol. 1, 243, 2012.
148. Zvoleff, A., https://cran.r-project.org/web/packages/glcm/glcm.pdf, 2016.
149. Segovia, F., et al., *Curr. Alzheimer Res.*, Vol. 13, 831, 2016.
150. Pham, V., et al., *Annual International Conference of the IEEE Engineering in Medicine and Biology Society*, 4791, IEEE, New York, 2009.
151. Parot, V., et al., *Magn. Reson. Med.*, Vol. 68, 17, 2012.
152. Frigo, G., et al., *International Symposium on Medical Measurements And Applications (MEMEA)*, 313, IEEE, Lisbon, Portugal, 2014.
153. He, T., et al., *Neurocomputing*, Vol. 174, 1049, 2016.
154. Gouid, G. G. N., et al., *IEEE Conference on Computational Intelligence in Bioinformatics and Computational Biology*, 7, 2014.
155. Srinivasan, S. V., et al., *Artificial Intelligence and Evolutionary Algorithms in Engineering Systems*, L. P. Suresh, et al. (eds,), Vol. 2, 687, Springer-Verlag Berlin, Berlin, 2015.
156. Tylki-Szymanska, A., et al., *Neuropediatrics*, Vol. 45, 188, 2014.
157. Nardone, R., et al., *J. Neuroimaging*, Vol. 20, 204, 2010.
158. Canneti, B., et al., *Rev. Neurologia*, Vol. 57, 354, 2013.
159. Campanella, M., et al., *Peer J*, Vol. 2, e497, 2014.
160. Bullitt, E., et al., *Methods*, Vol. 43, 29, 2007.
161. Karakasis, E. G., et al., *Pattern Recognit. Lett.*, Vol. 55, 22, 2015.
162. Bjork, G., et al., *Phys. Rev. A*, Vol. 85, 053835, 2012.
163. Zunic, J., et al., *Mach. Vis. Appl.*, Vol. 27, 129, 2016.
164. Marengo, E., et al., *2-D PAGE Map Analysis: Methods and Protocols*, E. Marengo, et al. (eds.), 271, Springer, New York, 2016.
165. Nayak, D. R., et al., *Neurocomputing*, Vol. 177, 188, 2016.
166. Wang, S., et al., *2nd National Conference on Information Technology and Computer Science (CITCS2015)*, A. Hu (ed.), 450, DEStech Publications, Inc., Lancaster, USA, 2015.
167. Das, A. B., et al., *Signal Image Video Process.*, Vol. 10, 259, 2016.
168. Han, R. X., et al., *Measurement Technology and Its Application*, P. Yarlagadda, et al. (eds.), Pts. 1 and 2, 974, Trans Tech Publications Ltd, Stafa-Zurich, 2013.
169. Najafizade, S. A., et al., *Chin. Phys. B*, Vol. 25, 040301, 2016.
170. Rioul, O., et al., *Bayesian Inference and Maximum Entropy Methods in Science and Engineering*, A. Mohammad Djafari, et al. (eds.), 105, Amer. Inst. Physics, Melville, 2015.
171. Mora, T., et al., *Phys. Rev. E*, Vol. 93, 052418, 2016.
172. Aptekarev, A. I., et al., *Eur. Phys. J. B*, Vol. 89, 85, 2016.
173. Senapati, D., et al., *Digit. Signal Prog.*, Vol. 48, 276, 2016.
174. Bhandari, A. K., et al., *Expert Syst. Appl.*, Vol. 42, 8707, 2015.
175. Mokni, R., et al., *J. Inf. Assur. Secur.*, Vol. 11, 77, 2016.
176. Malegori, C., et al., *J. Food Eng.*, Vol. 185, 48, 2016.

177. Yousefi Banaem, H., et al., *Iranian Journal of Radiology*, Vol. 12, e11656, 2015.
178. Fathima, M. M., et al., *International Conference on Information Communication and Embedded Systems*, 809, IEEE, Chennai, India, 2013.
179. Haralick, R. M., et al., *IEEE Transactions on Systems, Man, and Cybernetics*, 610, 1973.
180. James, A. P., et al., *IEEE Trans. Very Large Scale Integr.*, Vol. 23, 2690, 2015.
181. Shih, C.-C., *Optics Communications*, Vol. 118, 495, 1995.
182. Ozaktas, H. M., et al., *IEEE Transactions on Signal Processing*, Vol. 44, 2141, 1996.
183. Pei, S.-C., et al., *Optics Letters*, Vol. 22, 1047, 1997.
184. Liu, Y. N., et al., *Pattern Anal. Appl.*, Vol. 19, 369, 2016.
185. Erguzel, T. T., et al., *Comput. Biol. Med.*, Vol. 64, 127, 2015.
186. Maldonado, S., et al., *Intell. Data Anal.*, Vol. 19, 1259, 2015.
187. Mudali, D., et al., *Comput. Math. Method Med.*, 136921, 2015.
188. Shi, J. H., et al., *J. Stat. Plan. Infer.*, Vol. 175, 87, 2016.
189. Washizawa, Y., *IEICE Trans. Inf. Syst.*, Vol. E99D, 1353, 2016.
190. Thida, M., et al., *IEEE T. Cybern.*, Vol. 43, 2147, 2013.
191. Yang, B., et al., *Pattern Recognit.*, Vol. 55, 215, 2016.
192. Nguyen, V., et al., *Appl. Comput. Rev.*, Vol. 15, 17, 2015.
193. Weinberger, K. Q., et al., *Int. J. Comput. Vis.*, Vol. 70, 77, 2006.
194. Pulkkinen, S., *Optim. Method Softw.*, Vol. 30, 1050, 2015.
195. Hong, C. Q., et al., *Signal Process.*, Vol. 124, 132, 2016.
196. Jiang, J. F., et al., *Teh. Vjesn.*, Vol. 23, 77, 2016.
197. Ueda, Y., et al., *J. Signal Process. Syst. Signal Image Video Technol.*, Vol. 82, 151, 2016.
198. Yang, Y., et al., *Mach. Learn.*, Vol. 74, 39, 2009.
199. Merentitis, A., et al., *IEEE J. Sel. Top. Appl. Earth Observ. Remote Sens.*, Vol. 7, 1089, 2014.
200. Corander, J., et al., *Stat. Comput.*, Vol. 23, 59, 2013.
201. Kothandan, R., *Bioinformation*, Vol. 11, 6, 2015.
202. Torgo, L., et al., *Expert Syst.*, Vol. 32, 465, 2015.
203. Yin, Q. Y., et al., *Math. Probl. Eng.*, 761814, 2013.
204. Siers, M. J., et al., *Inf. Syst.*, Vol. 51, 62, 2015.
205. Mustafa, G., et al., *10th Iberian Conference on Information Systems and Technologies (CISTI)*, A. Rocha, et al. (eds.), 6, IEEE, Agueda, Portugal, 2015.
206. Ren, Y. F., et al., *Chin. J. Electron.*, Vol. 24, 52, 2015.
207. Smith, M. R., et al., *International Joint Conference on Neural Networks*, 2690, IEEE, San Jose, CA, USA, 2011.
208. Sun, J. W., et al., *Proceedings of Future Generation Communication and Networking*, 243, IEEE Computer Soc., Los Alamitos, 2007.
209. Saiyin, X. R. G., et al., *Proceedings of the 3rd International Conference on Mechatronics and Industrial Informatics*, S. B. Choi (ed.), 704, Atlantis Press, Paris, 2015.
210. Kinaci, A. C., et al., *22nd International Conference on Neural Information Processing*, S. Arik, et al. (eds.), 440, Springer Int. Publishing Ag, Istanbul, Turkey, 2015.
211. Zhao, J. L., et al., *Web Information Systems and Mining*, Z. Gong, et al. (eds.), 251, Springer-Verlag Press, Berlin, 2011.
212. Prossegger, M., et al., *Adaptive and Intelligent Systems*, A. Bouchachia (ed.), 182, Springer Int. Publishing Ag, Cham, 2014.
213. Yang, B. S., et al., *Advances in Knowledge Discovery and Data Mining, Proceedings*, T. Washio, et al. (eds.), 405, Springer-Verlag Berlin, Berlin, 2008.
214. Jin, H. X., et al., *IEEE International Conference on Automation and Logistics*, 359, IEEE, Electron Devices Soc. & Reliability Group, New York, 2007.

215. Zhu, W. T., et al., *International Joint Conference on Neural Networks*, 800, IEEE, New York, 2014.
216. Singh, L., et al., *Neural Information Processing*, S. Arik, et al. (eds.), Pt. I, 302, Springer Int. Publishing Ag, Cham, 2015.
217. Alom, M. Z., et al., *International Joint Conference on Neural Networks*, 1, IEEE, New York, 2015.
218. Singh, R. P., et al., *11th International Conference on Intelligent Information Hiding and Multimedia Signal Processing (IIH-MSP)*, J. Pan, et al. (eds.), 393, Adelaide, Australia, 2015.
219. Barreto, G. A., et al., *Neurocomputing*, Vol. 176, 3, 2016.
220. Aldahoul, N., et al., *Adv. Sci. Lett.*, Vol. 21, 3489, 2015.
221. Liu, T. C., et al., *18th International Conference on Intelligent Transportation Systems*, 1323, IEEE, Spain, 2015.
222. Lu, S., et al., *Multimedia Tools and Applications*, doi: 10.1007/s11042-016-3559-z, 2016.
223. Sun, J. Y., *Neurocomputing*, Vol. 79, 158, 2012.
224. Nurcahyo, S., et al., *2nd International Conference on Information and Communication Technology (ICOICT)*, 166, IEEE, Bandung, Indonesia, 2014.
225. Dunea, D., et al., *1st International Work-Conference on Time Series (ITISE)*, I. R. Ruiz, et al. (eds.), 804, Granada, Spain, 2014.
226. Chen, X. Y., et al., *Water Resour. Manag.*, Vol. 30, 2179, 2016.
227. Karami, A., *J. Netw. Comput. Appl.*, Vol. 56, 1, 2015.
228. Nienhold, D., et al., *3rd International Symposium on Computational And Business Intelligence*, S. Deb, et al. (eds.), 6, IEEE, Bali, Indonesia, 2015.
229. Jiao, L. M., et al., *Symbolic and Quantitative Approaches to Reasoning with Uncertainty*, S. Destercke, et al. (eds.), 461, Springer-Verlag, Berlin, 2015.
230. Liu, C. M., et al., *Advances in Knowledge Discovery and Data Mining*, T. Cao, et al. (eds.), Part I, 176, Springer-Verlag Berlin, Berlin, 2015.
231. An, F. W., et al., *Jpn. J. Appl. Phys.*, Vol. 55, 04ef10, 2016.
232. Dai, L. Z., et al., *4th National Conference on Electrical, Electronics and Computer Engineering*, J. Wang, et al. (eds.), 463, Atlantis Press, Paris, 2016.
233. Xie, Y., *Hybrid Intelligent Systems*, A. Abraham, et al. (eds.), 13, Springer-Verlag, Berlin, 2016.
234. Shi, J. Y., et al., *Intelligence Science and Big Data Engineering: Big Data and Machine Learning Techniques*, X. He, et al. (eds.), 477, Springer Int. Publishing Ag, Cham, 2015.
235. Mihaljevic, B., et al., *Advances in Artificial Intelligence, Caepia 2013*, C. Bielza, et al. (eds.), 159, Springer-Verlag Berlin, Berlin, 2013.
236. Kwon, W. Y., et al., *IEEE/RSJ International Conference on Intelligent Robots And Systems*, 3141, IEEE, Chicago, IL, 2014.
237. Krawczyk, B., et al., *International Conference on Systems, Man and Cybernetics*, 2147, IEEE Computer Soc, Los Alamitos, 2015.
238. Benadit, P. J., et al., *Proceedings of the International Conference on Information and Communication Technologies, ICICT 2014*, P. Samuel (ed.), 184, Elsevier Science Bv, Amsterdam, 2015.
239. Mohan, D., et al., *2nd International Conference on Communication Systems*, K. Singh, et al. (eds.), 17, Amer. Inst. Physics, Melville, 2016.
240. Ling, P., et al., *International Joint Conference on Neural Networks*, 438, IEEE, Beijing, Peoples R. China, 2014.
241. Lu, B. L., et al., *Proceedings of the 4th International Conference on Mechatronics, Materials, Chemistry and Computer Engineering 2015*, Z. Liang, et al. (eds.), 31, Atlantis Press, Paris, 2015.
242. Stylios, C. D., et al., *XIV Mediterranean Conference on Medical and Biological Engineering and Computing 2016*, E. Kyriacou, et al. (eds.), 1205, Springer, New York, 2016.
243. Na, W., et al., *5th International Conference on Advanced Computational Intelligence*, 686, IEEE, Nanjing, Peoples R. China, 2012.

244. Xie, X. J., et al., *International Joint Conference on Neural Networks*, 1, IEEE, Killarney, Ireland, 2015.
245. Dufrenois, F., et al., *International Joint Conference on Neural Networks*, 12, IEEE, Killarney, Ireland, 2015.
246. Arumugam, P., et al., *International Conferenced on Circuits, Power and Computing Technologies (ICCPCT)*, 5, IEEE, Nagercoil, India, 2015.
247. Maeda, T., et al., *International Conference on Image Processing*, 5177, IEEE, New York, 2014.
248. Wang, S., et al., *Progress In Electromagnetics Research*, Vol. 144, 171–184, 2014.
249. Kallas, M., et al., *Pattern Recognit.*, Vol. 46, 3066, 2013.
250. Hejazi, M., et al., *Digit. Signal Prog.*, Vol. 52, 72, 2016.
251. Mandavi, S., et al., *Inf. Sci.*, Vol. 295, 407, 2015.
252. Mashwani, W. K., et al., *Int. J. Adv. Comput. Sci. Appl.*, Vol. 7, 583, 2016.
253. Reina, D. G., et al., *Int. J. Distrib. Sens. Netw.*, 2082496, 2016.
254. Jaiyeola, A. T., et al., *Nat. Resour. Model.*, Vol. 28, 207, 2015.
255. Chong, C. K., et al., *Curr. Bioinform.*, Vol. 9, 509, 2014.
256. Claveria, O., et al., *East. Eur. Econ.*, Vol. 54, 171, 2016.
257. Zhang, Y., et al., *Expert Syst.*, Vol. 33, 239, 2016.
258. Ji, G., et al., *Entropy*, Vol. 17, 5711, 2015.
259. Wang, S., et al., *Simulation*, Vol. 92, 637, 2016.
260. Pereyra, M., et al., *IEEE J. Sel. Top. Signal Process.*, Vol. 10, 224, 2016.
261. Kovacevic, R. M., et al., *Eur. J. Oper. Res.*, Vol. 237, 389, 2014.
262. Agapie, A., *Business Excellence Challenges during the Economic Crisis*, C. Bratianu, et al. (eds.), 1, Editura Univ. Transilvania Brasov, Romania, Brasov, 2012.
263. Suzuki, S., *Eur. Phys. J.-Spec. Top.*, Vol. 224, 51, 2015.
264. Elsayed, S., et al., *Int. J. Comput. Intell. Appl.*, Vol. 14, 1550025, 2015.
265. Afshar, A., et al., *Water Resour. Manag.*, Vol. 29, 3891, 2015.
266. Ji, G., *Math. Probl. Eng.*, 931256, 2015.
267. Akay, B., et al., *Signal Image Video Process.*, Vol. 9, 967, 2015.
268. Kisi, O., et al., *Appl. Math. Comput.*, Vol. 270, 731, 2015.
269. Patnaik, L. M., et al., *Biomedical Signal Processing and Control*, Vol. 1, 86, 2006.
270. El-Dahshan, E. S. A., et al., *Digit. Signal Prog.*, Vol. 20, 433, 2010.
271. Dong, Z., et al., *Expert Syst. Appl.*, Vol. 38, 10049, 2011.
272. Wu, L., *Progress In Electromagnetics Research*, Vol. 130, 369–388, 2012.
273. Saritha, M., et al., *Pattern Recognit. Lett.*, Vol. 34, 2151, 2013.
274. Das, S., et al., *Progress in Electromagnetics Research*, Vol. 137, 1, 2013.
275. Dong, Z., et al., *Entropy*, Vol. 17, 1795, 2015.
276. Zhou, X., et al., *Bioinformatics and Biomedical Engineering*, F. Ortuño, et al. (eds.), 201, Springer International Publishing, Granada, Spain, 2015.
277. Feng, C., et al., *Int. J. Imaging Syst. Technol.*, Vol. 25, 153, 2015.
278. Phillips, P., et al., *Progress In Electromagnetics Research*, Vol. 152, 41–58, 2015.
279. Sun, P., et al., *Bio-medical Materials and Engineering*, Vol. 26, 1283, 2015.
280. Dong, Z., et al., *J. Med. Imaging Health Inform.*, Vol. 5, 1395, 2015.
281. Yang, X.-J., et al., Springer Plus, Vol. 4, 716, 2015.
282. Yang, X., et al., *Entropy*, Vol. 17, 8278, 2015.
283. Du, S., et al., *Multimedia Tools and Applications*, doi: 10.1007/s11042-016-3401-7, 2016.
284. Zhou, X.-X., et al., *Simulation*, doi: 10.1177/0037549716629227, 2016.
285. Lu, S., et al., *Applied Sciences*, Vol. 6, 169, 2016.

286. Wang, S., et al., *Biomedical Engineering/Biomedizinische Technik*, doi: 10.1515/bmt-2015-0152, 2016.
287. Sun, Y., et al., *J. Med. Syst.*, Vol. 40, 173, 2016.
288. Johnson, D. M., et al., *IEEE Trans. Knowl. Data Eng.*, Vol. 28, 1035, 2016.
289. Araujo, B., et al., *Expert Syst. Appl.*, Vol. 45, 234, 2016.
290. Vong, W. K., et al., *Psychon. Bull. Rev.*, Vol. 23, 230, 2016.
291. Bloom, V., et al., *Comput. Vis. Image Underst.*, Vol. 144, 62, 2016.
292. Tang, J., et al., *ACM Trans. Inf. Syst.*, Vol. 34, 7, 2016.
293. Shi, L. Y., et al., *Sci. Rep.*, Vol. 6, 22804, 2016.
294. Chen, Y., et al., *IEEE Trans. Image Process.*, Vol. 25, 988, 2016.
295. Wang, S., et al., *Comput. Math. Method Med.*, Vol. 454076, 2015.
296. Zhang, Y., et al., *Sensors*, Vol. 11, 4721, 2011.
297. Alijla, B. O., et al., *Inf. Sci.*, Vol. 325, 175, 2015.
298. Zhang, Y., *Expert Syst. Appl.*, Vol. 36, 8849, 2009.
299. Sheta, A. F., et al., *Int. J. Adv. Comput. Sci. Appl.*, Vol. 7, 499, 2016.
300. Klein, C. E., et al., *IEEE Trans. Magn.*, Vol. 52, 7208304, 2016.